HEFAT2011
8th International Conference on Heat Transfer, Fluid Mechanics and Thermodynamics
11-13 July 2011
Pointe Aux Piments, Mauritius

Heat Transfer Coefficients for Laminar to Turbulent Flow in Tubes at Constant Heat Flux

JP Meyer and M Hallquist
Department of Mechanical and Aeronautical Engineering, University of Pretoria,
Pretoria, 0002, South Africa

ABSTRACT

Due to constraints and changes in operating conditions, heat exchangers are often forced to operate under conditions of transitional flow. However, the heat transfer and flow behavior in this regime is relatively unknown. By describing the transitional characteristics it would be possible to design heat exchangers to operate under these conditions and improve the efficiency of the system. This study was aimed at obtaining experimental data for water flowing through a smooth tube with an inner diameter of 8 mm under constant heat flux conditions. Four heat flux test cases were considered namely: 1 409, 3 354, 5 009 and 6 881 W/m^2. The experiments covered a Reynolds number range of 500 to 8 800, a Prandtl number range of 4 to 7, a Nusselt number range of 6 to 67, and a Grashof number range of 750 to 25 600. Experiments have shown a smooth transition from laminar to turbulent flow.

Keywords: *smooth tube, constant heat flux, transition, heat transfer coefficients*

INTRODUCTION

A good design of a heat exchanger should consider methods of increasing heat transfer performance whilst reducing the pressure drop [1].

It is accepted in literature that the transition from laminar to turbulent flow occurs at a Reynolds number of 2300 [2]. Turbulent flow provides the best heat transfer coefficients with the disadvantage of high pressure drops, whereas the opposite is true for laminar flow. The alternative is to consider transitional flow, which would provide better heat transfer characteristics than laminar flow with lower pressure drops compared to turbulent flow.

However, it is uncommon to design heat exchangers that operate in the transitional flow regime due to the perceived chaotic behavior of the flow and the insufficient information available for this regime [3].

The aim of this paper is to obtain heat transfer data for the transitional regime for water flowing through a smooth tube under constant heat flux conditions.

NOMECLATURE

A	[m^2]	Area
C_p	[J/kgK]	Specific heat
d_i	[m]	Inner tube diameter
d_o	[m]	Outer tube diameter
f	-	Friction factor
h	[W/m^{2}K]	Heat transfer coefficient
i	[A]	Current
k	[W/mK]	Thermal conductivity
L	[m]	Length
$\dot{m}$	[kg/s]	Mass Flow
Nu	-	Nusselt number
Q	[W]	Heat transfer
Q_{elec}	[W]	Electric power
q	[W/m^2]	Heat flux
R	[Ω]	Electrical resistance
R_o	[Ω]	Reference resistance
$R_{thermal}$	[K/W]	Thermal resistance
Re	-	Reynolds number
T	[ºC]	Temperature
T_{so}	[ºC]	Outer surface temperature
T_{si}	[ºC]	Inner surface temperature
T_b	[ºC]	Bulk fluid temperature
T_f	[ºC]	Fluid temperature
v	[m/s]	Velocity
V	[V]	Voltage Potential
x	-	Position
α	[Ωm/K]	Temperature coefficient
σ	[Ωm]	Electrical resistivity
ρ	[kg/m^3]	Density
μ	[kg/ms]	Dynamic viscosity
β	[1/K]	Volume expansivity
η	[%]	Efficiency
ν	[m^2/s]	Kinematic viscosity
Δ	-	Difference/change

EXPERIMENTAL SET UP

The overall test set up (Figure 1) consisted of a closed water loop that circulates water from a storage tank through a removable test section back to the storage tank. This test section is set up to accommodate test tubes of different diameters and lengths. Various heat fluxes could be applied to the test section by passing different currents through the

test tubes. The heat fluxes considered in this case were 1 409, 3 354, 5 009 and 6 881 W/m^2.

Water was supplied from a storage tank to the test section by means of a positive displacement pump which is used in conjunction with a speed controller to maintain a selected volume flow rate. Two coriolis flow and density meters with different ranges were installed in parallel to be used in accordance with the flow rate requirements.

The water in the storage tank was connected to a chiller that maintained the temperature in the storage tank to approximately 20˚C (temperature ranged from 18.5°C to 21.5°C).

A direct current arc welder was used to feed current to the test section where the current was controlled by a modular prediction control (MPC) controller. The controller ensured the product of the voltage and current remained constant to ensure a constant heat flux to the test section.

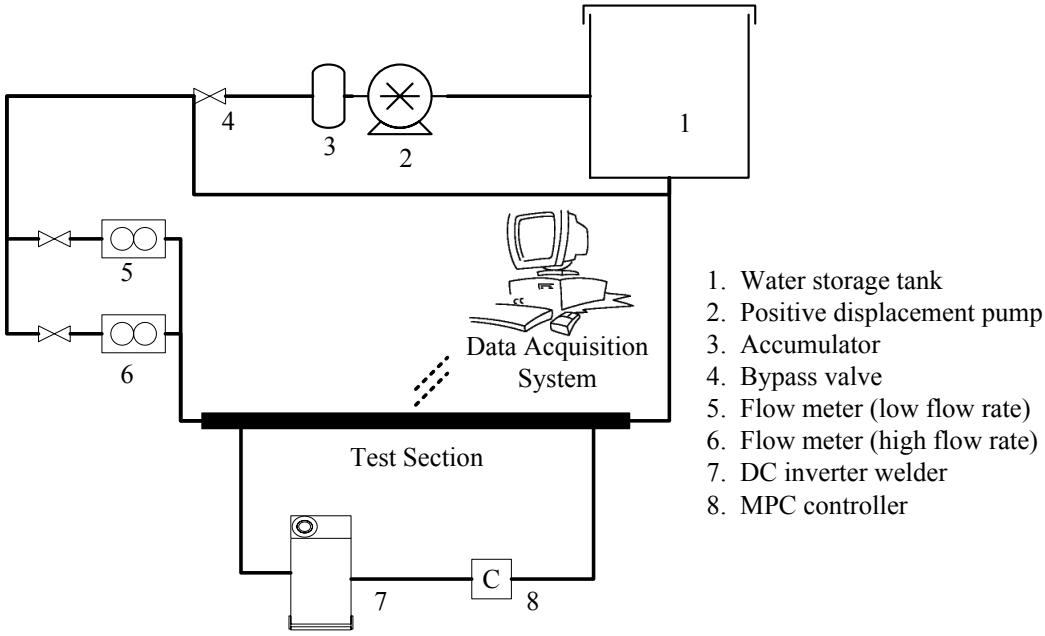

Figure 1: Experimental Set Up

The test section (Figure 2) consisted of an insulated stainless steel tube with an inner diameter of 8 mm and a length of 5.7 m. T-type thermocouples were attached to the tube with thermal epoxy for the temperature measurements. All the thermocouples used in these experiments were calibrated to an accuracy of approximately 0.1°C.

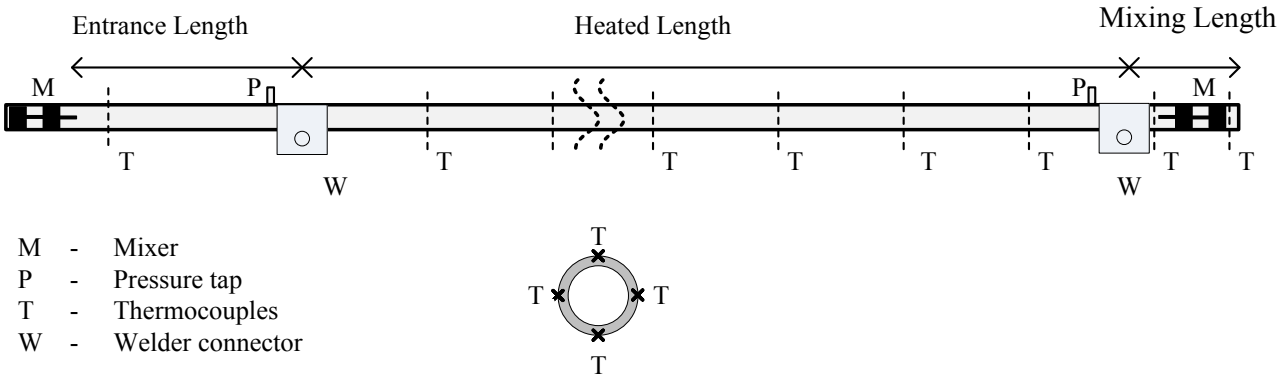

Figure 2: Test Section

Four thermocouples were used at each station and the thermocouples were attached to the top, bottom and sides (90˚ from each other) of the test section tubes at 15 stations along the length of the tube (60 thermocouples in total).

At the inlet and outlet the four thermocouple readings were averaged to get the average water inlet and outlet temperatures respectively. Mixers were inserted at the inlet and outlet of the test section to ensure no temperature gradients existed, especially during laminar and transitional

flow experiments. Measurements were only taken after the mixers at the inlet and the outlet so that the wall temperatures would approximate the average fluid temperature.

The measurement ranges considered a Reynolds number range of 500 to 8 800. The associated Nusselt number was between 6 and 67, with the Grashoff number ranging from 750 to 25 600 and the Prandtl number from 4 to 7.

An uncertainty analysis performed on the system with respect to measured and calculated parameters provided an accuracy of 0.51% for the heat transfer coefficients and 1% on the Reynolds number.

DATA REDUCTION

Heat transfer was achieved through the heating effect of the electrical power (Q_{elect}) delivered to the system, which was determined from the measured current *(i)* and the electrical resistance (R) of the test section as follows:

$$Q_{elec} = i^2 R \tag{1}$$

The electrical resistance (R) of the test section was determined by the following correlation which is a function of the average test section temperature and the temperature coefficient (α) of stainless steel, obtained from the material certificate of the supplier (Eurosteel):

$$R = R_0[\alpha(T - T_0) + 1] \tag{2a}$$

where

$$R_0 = \sigma \frac{L}{A} \tag{2b}$$

The reference resistance (R_o) in the equation is the resistance at a temperature (T_o) of 20˚C, where L is the heated length of the test tube and A is the cross sectional area of the tube material. From this the resistance can be calculated from:

$$V = iR \tag{3}$$

The inside wall temperatures (T_{si}) were determined by subtracting the temperature drop, as a result of the wall resistance, from the measurements of the outside wall temperatures (T_{so}):

$$T_{si} = T_{so} - \frac{Q_{elec}}{R_{thermal}} \tag{4a}$$

where

$$R_{thermal} = \frac{\ln(d_o / d_i)}{2\pi k L} \tag{4b}$$

The heat input from the electricity side (Q_{elec}) was used in equation 4a because the local heat input could be directly determined as opposed to the heat transfer on the water side which is solely dependent on the inlet and outlet temperatures.

The wall thickness of the test sections were approximately 1 mm and thermal conductivity is quite high resulting in a maximum temperature drop of 0.33 °C across the tube wall.

The average fluid temperature at any point, x, along the tube was determined from

$$T_f(x) = T_{f,i} + \frac{q(x)\pi d_i x}{\dot{m} Cp(x)} \tag{5}$$

where $q(x)$ is determined from the local heat flux based on the current passing through the test section and the local electrical resistance $R(x)$ between the inlet and point x. $R(x)$ is determined from equation 2 above where the temperature is the average wall temperature between the inlet and point x.

The heat flux was determined as

$$q(x) = \frac{Q(x)}{\pi d_i x} \tag{6}$$

This equation is solved in an iterative manner where the specific heat is initially based on the average between the inlet temperature and the wall temperature at point x. Once the fluid temperature at position x has been calculated, the specific heat is adjusted according to this temperature until convergence has been achieved.

This process was repeated for each station after which the last element was compared to the actual measured outlet temperature. The difference between the numerical analysis and the measured temperature is directly related to the error between the power input to the system and the heat transfer between the water inlet and outlet. This error ranges from 1.4°C at low Reynolds numbers to 0.11°C at high Reynolds number.

The results of the calculated fluid temperature illustrated a straight line profile between inlet and calculated outlet as is expected for a constant heat flux boundary condition. The tube inner wall temperatures and the average fluid temperatures were used to determine the heat transfer coefficient and ultimately the Nusselt number. The average heat transfer coefficient for the entire test section was determined as

$$\bar{h} = \frac{q_s}{\overline{T_s} - T_b} \tag{10}$$

The average wall temperature $\overline{T_s}$ is determined by integrating the average of the 14 measurement stations along the length of the tube using the trapezoidal rule

$$\overline{T}_s = \frac{1}{22}\left\{T_{s1} + 2\sum_{2}^{13} T_{sx} + T_{s14}\right\} \tag{11}$$

The bulk temperature in Equation 9 was determined as the average temperature between the fluid inlet bulk temperature and outlet bulk temperature, thus.

$$T_b = \frac{T_{fi} - T_{fo}}{2} \tag{12}$$

The average Nusselt number was then determined as

$$\overline{Nu} = \frac{\bar{h} d_i}{\bar{k}} \tag{13}$$

where the average thermal conductivity $\bar{k}$ was based on the bulk fluid temperature as calculated by equation 12. The corresponding average Reynolds number was determined as

$$\overline{Re} = \frac{4\dot{m}}{\pi \mu d_i} \tag{14}$$

where the viscosity was determined at the bulk temperature (equation 12).

RESULTS

The measurements of the 3 354 W/m^2 case were compared to both the Ghajar and Tam correlation [4, 5] and the Gnielinski [6, 7] correlation.

The results are shown in Figure 3. These results demonstrate that the Nusselt number does not remain constant in the laminar regime transitions smoothly from laminar to turbulent flow. The Ghajar correlation also predicts a varying Nusselt number in the laminar regime, however, the measured results are consistently higher (ranging from 1.6 at a Reynolds number of 2 000 to 2.5 at a Reynolds number of 1 000).

.

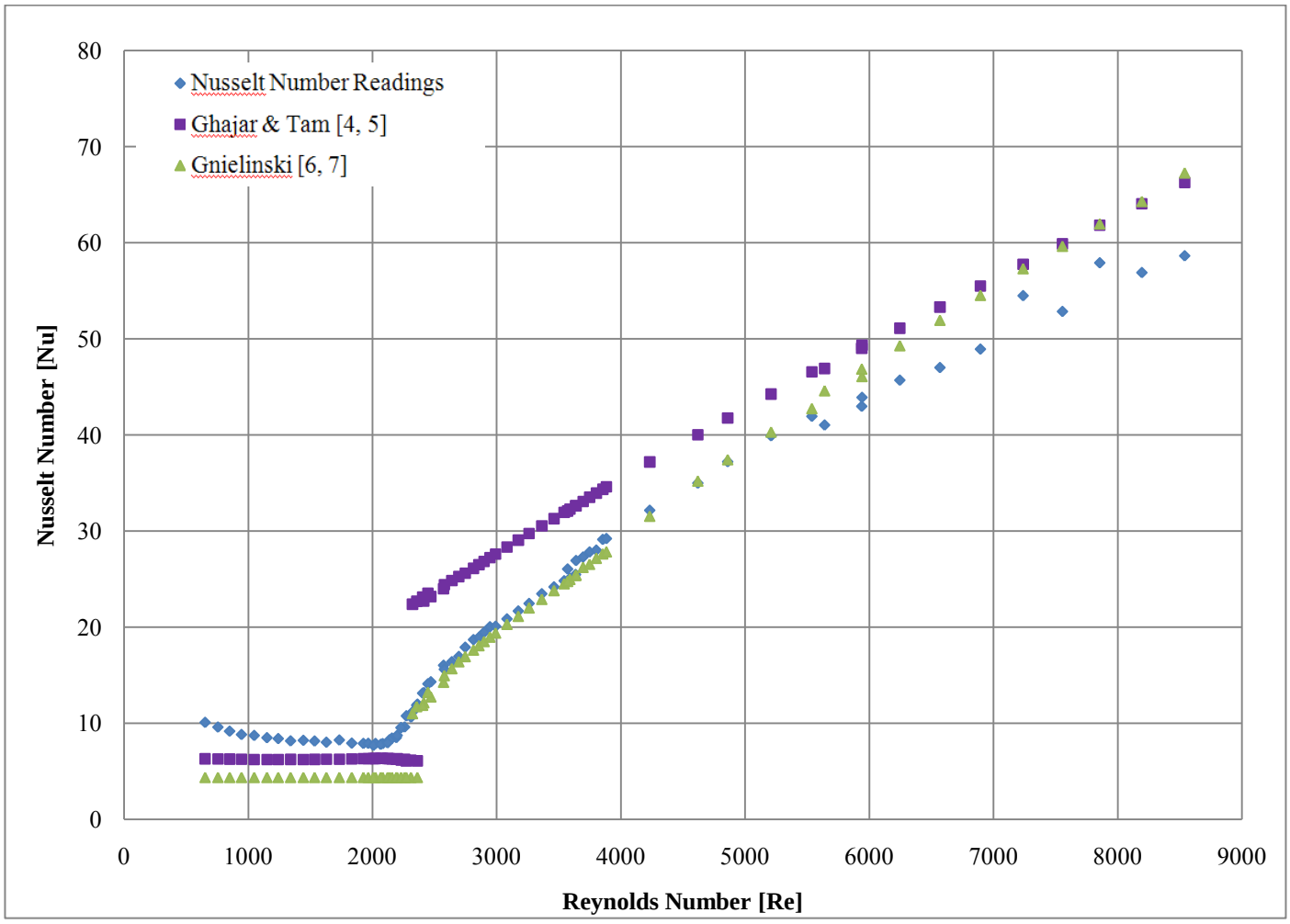

Figure 3: Results of 3 354W/m^2 case plotted with Ghajar correlation [4, 5]

Transition from laminar to turbulent flow occurs between Reynolds number of 2 080 and 2 500, which corresponds to the transition measured with the pressure drops. This transition is quite steep but does follow a smooth profile.

The turbulent results resemble those predicted by Gnielinski after reaching a Reynolds number of approximately 3 300. At higher Reynolds numbers (7 000) it appears that the Gnielinski and Ghajar correlations merge, as do the results. Most correlations for turbulent flow are specified for Reynolds numbers higher than 10 000 which suggests lower accuracies of the correlations at lower Reynolds values. The close correspondence of the results at turbulent flow proves the validity of the test set up (within 10 % of the Ghajar correlation at a Reynolds number of 5 000).

The average Nusselt number for the 10 mm tube is shown Figure 4. In the laminar regime the Nusselt number increases from a value of approximately 6 for a heat flux of 1 409 W/m^2 to 10 at 6 881 W/m^2. As the flow rate decreases to zero, the Nusselt number increases slightly, this is attributed to the increased heat lost through the insulation at low flow rates.

Transition from laminar to turbulent flow occurs between Reynolds numbers of 2 100 and 2 300. As the heat flux increases the transition to turbulence is delayed with the onset of transition for the 1 409 W/m^2 occurring at a Reynolds number of 2 050, 2 130 for the 3 354 W/m^2 case, 2 180 for the 5 009 W/m^2 case and finally at a Reynolds number of 2 280 for the highest heat flux case. The gradient of transition is the same in each case. At a Reynolds number of approximately 3 000 the gradient of the Nusselt number changes, marking the end of transition.

In the turbulent flow regime, the Nusselt number is higher for increased heat fluxes. The results of the 1 409 W/m^2 break away from the other results at a Reynolds number of 3 400 increasing at a much smaller gradient than the other results.

At high Reynolds numbers "scattering" occurs in the measured Nusselt number due to increasing uncertainties.

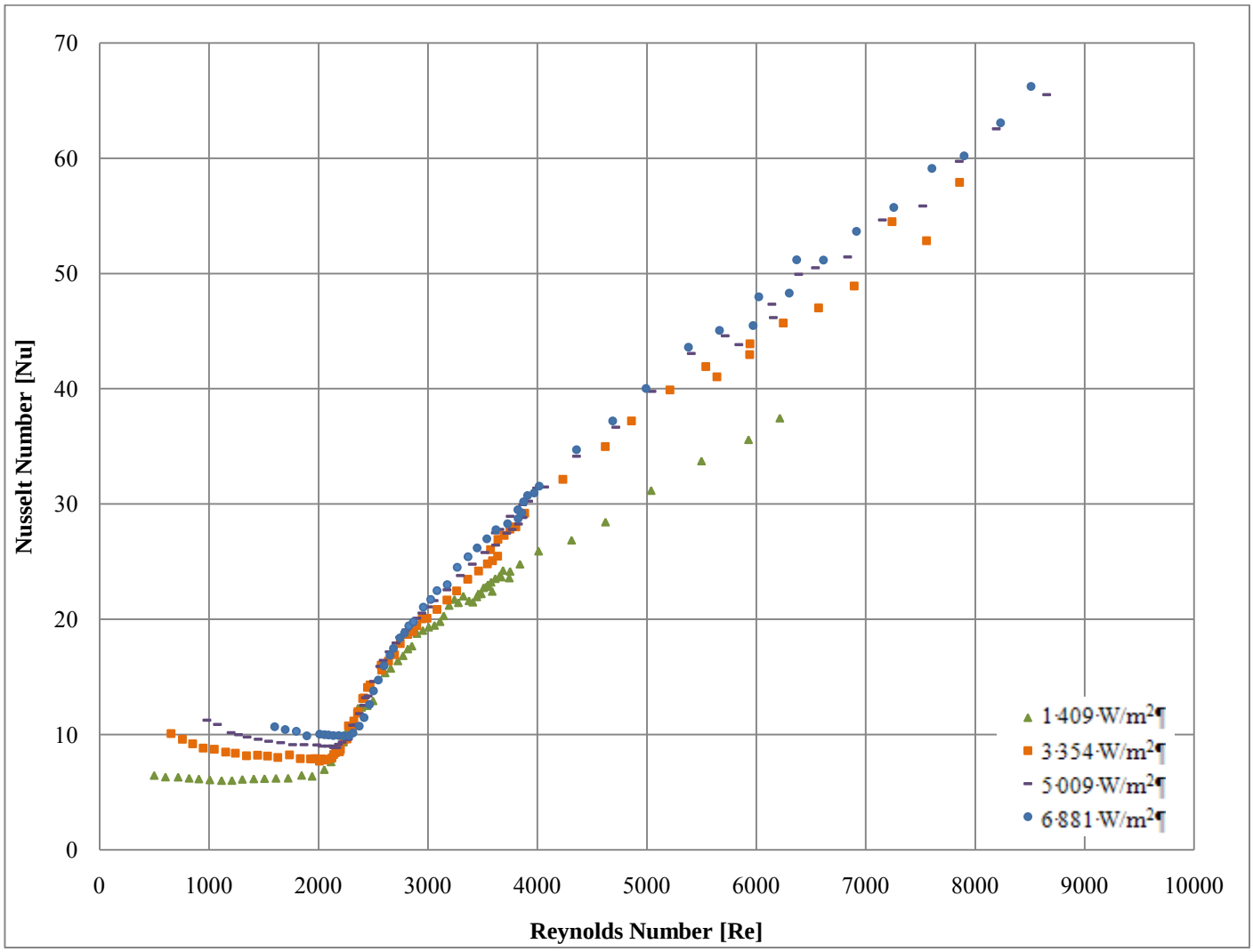

Figure 4: Results for all test cases

CONCLUSIONS

A smooth transition from laminar to turbulent flow was illustrated, as opposed to chaotic behavior predicted in theory. The Reynolds number marking the onset of transition has been shown to be dependent on the heat flux of the system. As the heat flux is increased, the onset of transition is delayed.

The smooth transition profile shown, suggests the potential to develop useful correlations for this region that can be used to design heat exchangers for transitional flow.

REFERENCES

1. **Shokouhmand H and Salimpour MR** Optimal Reynolds Number of Laminar Forced Convection in a Helical Tube Sunject to Uniform Wall Temperature: International Communications in Heat & Mass Transfer, 2007. - Vol. 34. - pp. 753-761.
2. **ASHRAE,** Fluid Flow, ASHRAE Handbook – Fundamentals, American Society of Heating, Refrigerating and Air-Conditioning Engineers, Inc., Atlanta, 2005.
3. **Olivier JA and Meyer JP** Single-Phase Heat Transfer and Pressure Drop of Cooling of Water inside Smooth Tubes for Transitional Flow with Different Inlet Geometries: HVAC & R Research, 2010. - 4 : Vol. 16. - pp. 471-496.
4. **Ghajar AJ and Tam LM** Heat Transfer Measurements and Correlations in the Transition Region for a Circular Tube with Three Different Inlet Configurations: Experimental Thermal & Fluid Sciences, 1994. - Vol. 8. - pp. 79-90.
5. **Ghajar AJ and Tam LP** Flow Regime Map for a Horizontal Pipe with a Uniform Wall Heat Flux & Three Inlet Configurations: Experimental Thermal & Fluid Sciences, 1995. - Vol. 10. - pp. 287-297.
6. **Gnielinski V** Heat Transfer Coefficients for Turbulent Flow in Concentric Annuli: Heat Transfer Engineering, 2009. - 6 : Vol. 30. - pp. 431-436.
7. **Gnielinski V** New Equations for Heat & Mass Transfer in Turbulent Pipe and Channel Flow: International Chemical Engineering, 1976. - 2 : Vol. 16. - pp. 359-368.